

Formation Control for UAVs Using a Flux Guided Approach

John Hartley¹, Hubert P. H. Shum², Edmond S. L. Ho¹, He Wang³ and Subramanian Ramamoorthy⁴

Abstract—While multiple studies have proposed methods for the formation control of unmanned aerial vehicles (UAV), the trajectories generated are generally unsuitable for tracking targets where the optimum coverage of the target by the formation is required at all times. We propose a path planning approach called the Flux Guided (FG) method, which generates collision-free trajectories while maximising the coverage of one or more targets. We show that by reformulating an existing least-squares flux minimisation problem as a constrained optimisation problem, the paths obtained are $1.5\times$ shorter and track directly toward the target. Also, we demonstrate that the scale of the formation can be controlled during flight, and that this feature can be used to track multiple scattered targets. The method is highly scalable since the planning algorithm is only required for a sub-set of UAVs on the open boundary of the formation's surface. Finally, through simulating a 3d dynamic particle system that tracks the desired trajectories using a PID controller, we show that the resulting trajectories after time-optimal parameterisation are suitable for robotic controls.

Index Terms—formation control, unmanned aerial vehicles, UAV, robotics, flux, trajectory, tracking

I. INTRODUCTION

Formation flying of unmanned aerial vehicles (UAV) has been of interest to researchers for the past two decades. A major reason is that in many applications, multiple UAVs can more easily accomplish tasks that are harder to achieve using a single robot. For example, multiple UAVs can improve autonomous navigation by working together to share power and multi-sensor hardware where the payload of the individual drones is limited [1]. Crucial to the operation of multiple UAVs is the ability to plan feasible trajectories that have non-colliding properties.

Tracking, and surrounding remote targets with a formation of robots is a useful application of formation flying for UAVs. Realistic applications include tracking and neutralisation of aerial threats, as well as search and rescue operations. Successful operation in these scenarios requires the formation to maximally face toward the target such that the target can be observed and surrounded more easily. In addition, the

geometry of the path taken by the UAVs should occupy a minimum volume such that the UAVs can operate within restrictive environments and move efficiently.

Several studies have used artificial potential fields (APF) to guide single agents through known environments [2]. Typically, attractive and repulsive potentials fields are constructed to represent the goal and obstacles in the environment respectively. The direction of travel of an agent is found by calculating the force on the agent using iterative gradient descent of the sum of the attractive and repulsive potentials [3]–[6]. Issues with local minima in the potential fields can be resolved by carefully constructing the potential functions such that a global minima at the target exists or by global optimisation methods such as simulated annealing [7]–[9].

APF methods have also been used for path planning for multiple agents moving in formation. A common approach is to develop a leader-follower relationship among the agents in the formation. The leader's motion is determined by the APF approach and the followers' are guided by the leader using a tracking or control mechanism. The positions of the follower agents can be determined by maintaining a separation distance and angle with respect to the motion of the leader [10], or by using additional potential fields for the leaders and followers [11]. These approaches can be vulnerable to the safety of the leader UAV. However, this issue has been mitigated using virtual [12] and implicit leaders [13].

The main drawback of the single leader approach is that the direction of motion of the leader also defines the orientation of the formation. In the case where we require the formation to face the target, this behaviour is problematic since a change in the direction of the leader causes large changes in the structure of the formation as the formation adapts to the new direction of travel. Without a feedback mechanism between the leaders and followers, the risk of collision is increased. This assignment problem has been solved in a distributed manner by [14]. However, the formation is forced to break down during the re-assignment. These methods do not ensure optimal coverage of the target.

A more advanced approach is presented in [15] where an open surface defined by a set of agents covers a target. The paths of the agents are solved by maximising the electric flux through an open surface defined by the topology of the agents, which are positioned in an electric field generated by a target charge. Collision free path is always obtained since the flux is sub-optimal or zero in the event of a collision. A limitation of the method is that the scale of the formation cannot be controlled. This leads to optimal coverage but at a very long range. As such this method is not suitable

*This work is supported by the MOD Chief Scientific Adviser's Research Programme, through the Defence and Security Accelerator (Ref: DSTLX-1000140725), and the Royal Society (Ref: IES\R2\181024 and IES\R1\191147)

¹John Hartley and Edmond S. L. Ho are with Department of Computer and Information Sciences, Northumbria University, Newcastle upon Tyne, UK john.hartley@northumbria.ac.uk and e.ho@northumbria.ac.uk

²Hubert P. H. Shum, the corresponding author, is with the Department of Computer Science, Durham University, Durham, UK hubert.shum@durham.ac.uk

³He Wang is with the School of Computing, University of Leeds, Leeds, UK h.e.wang@leeds.ac.uk

⁴Subramanian Ramamoorthy is with the School of Informatics, University of Edinburgh, Edinburgh, UK s.ramamoorthy@ed.ac.uk

when the target should be closely surrounded. Also, the paths generated by the method have been seen to be indirect and therefore inefficient for locating targets.

The contributions of the work are threefold. (1) We show that it is possible to control the scale of the formation using an additional term in the cost function given by [15]. (2) As the resulting paths are arc-shaped and therefore inefficient, we introduce a new formulation of the flux minimisation approach called the Flux Guided approach. Using this approach we show that the scale of the formation can be controlled, and more efficient paths towards the target can be derived. (3) We show that these paths are suitable for robotic control using a time re-parameterisation, and 3d dynamics particle simulation with a PID controller that tracks the desired trajectories.

II. FLUX OPTIMISATION FOR FORMATION TRAJECTORY PLANNING

In [15], a method is proposed for the problem in computer graphics of covering a target object with a cloak modelled using a collection of points acting under spring constraints. This is achieved using an iterative approach where the positions of the points are updated by requiring a positive change in the electric flux through the open surface of the cloak in the presence of an electric charge serving as a target. Collision free paths from the initial position of the points to the target positions are deduced since a collapse of the surface reduces the overall flux.

In this work, we extend this idea to the path planning problem of the formation of UAVs required to cover a target. We will refer to the original formulation in [15] as the least-squared flux (LS) approach. In this section, we give an overview of the LS method in terms of its application to the UAV formation planning problem. Firstly, we show the calculation for the flux (Section II-A) through the surface of the formation. Secondly, the update method is presented in Section II-B). Finally, we illustrate the novel property that the FG does not require the coordinates of every UAV in the formation in Section II-C.

A. Flux Evaluation

The first step in the LS method is to consider a formation under test and the surface it defines such that the flux can be calculated. Here, we adapt the methodology to fit with the goal of directing the formation of UAVs toward a target.

We demonstrate the LS and FG methods using a hemispherical formation in this work, while the approach permits any set of positions or number of UAV that form an open surface. Figure 1 shows the hemispherical formation used in this work. The formation consists of a 9 UAVs placed on a hemispherical surface of radius r . The points are denoted $\mathbf{p}_1, \mathbf{p}_2, \mathbf{p}_3, \mathbf{p}_4, \mathbf{f}_1, \mathbf{f}_2, \mathbf{f}_3, \mathbf{f}_4, \mathbf{f}_5$.

The points $\mathbf{p}_1, \mathbf{p}_2, \mathbf{p}_3, \mathbf{p}_4$ form a square which inscribes a circle of radius r . The surface of square is denoted S_1 and has a normal vector $\hat{\mathbf{n}}$. The points $\mathbf{f}_1, \mathbf{f}_2, \mathbf{f}_3, \mathbf{f}_4$ form a square which inscribe a circle translated a distance $\frac{r}{2}$ in the negative $\hat{\mathbf{n}}$ direction. The point \mathbf{f}_5 has a distance r

from the first circle in the negative $\hat{\mathbf{n}}$ direction. We define the closed surface of the formation, $S = S_1 + S_2$. Where S_2 is the curved surface, which passes through the points $\mathbf{p}_1, \mathbf{p}_2, \mathbf{p}_3, \mathbf{p}_4, \mathbf{f}_1, \mathbf{f}_2, \mathbf{f}_3, \mathbf{f}_4, \mathbf{f}_5$.

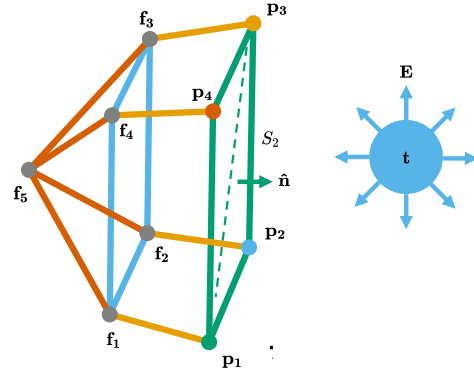


Fig. 1: Points on an open hemispherical surface representing a hemispherical surface. The target is a point charge at position \mathbf{t} . The surface S_1 is bounded by the points $\mathbf{p}_1, \mathbf{p}_2, \mathbf{p}_3, \mathbf{p}_4$.

The electric flux, Φ , through the hemispherical surface is given by:

$$\Phi = \iint_{S_2} \mathbf{E} \cdot \hat{\mathbf{n}} dA, \quad (1)$$

where \mathbf{E} is the electric field generated by the target, \mathbf{n} is a normal vector to the surface S_2 , and dA is an infinitesimal area on S_2 .

This integral can be solved directly. However, it is likely that the minimisation procedure will produce small deformations in the positions of the UAVs and thus the real S_2 is not always exactly hemispherical. The exact flux through the surface can be calculated by triangulating the surfaces between the UAVs and summing the flux through each triangle given by Equation 2 [16]:

$$\tan \frac{\Phi}{2} = \frac{(\mathbf{a} \times \mathbf{b}) \cdot \mathbf{c}}{|\mathbf{a}||\mathbf{b}||\mathbf{c}| + (\mathbf{a} \cdot \mathbf{b})|\mathbf{c}| + (\mathbf{a} \cdot \mathbf{c})|\mathbf{b}| + (\mathbf{b} \cdot \mathbf{c})|\mathbf{a}|} \quad (2)$$

where $\mathbf{a} = \mathbf{p} - \mathbf{A}$, $\mathbf{b} = \mathbf{p} - \mathbf{B}$, $\mathbf{c} = \mathbf{p} - \mathbf{C}$ and \mathbf{p} is the location of the target, and $\mathbf{A}, \mathbf{B}, \mathbf{C}$ are the position vectors of the vertices of triangle.

B. UAV Positions Updating

The geometric path of each UAV is found iteratively. Since we have a function of the flux in terms of the positions of the UAVs, we define a total differential that approximates the local change in flux with position:

$$\Delta \Phi = J_\phi \Delta x, \quad (3)$$

where $\Delta x = (\Delta x_{1_x}, \Delta x_{2_x}, \dots, \Delta x_{4_x}, \dots, \Delta x_{1_y}, \dots, \Delta x_{4_y})$ denotes a vector of the change in position of each UAV, J_ϕ is the Jacobian of the flux with respect to the changes in the positions of the UAVs.

Now, we define a Tikhonov regularized least-squares problem which minimises the error in the total differential and a target change in flux, ϕ_r , with a regularisation term, α is a soft constraint which increases the influence of the flux term:

$$J(\Delta x) = \Delta x^T \Delta x + \alpha(\phi_r - J_\phi \Delta x)^2 \quad (4)$$

C. Reducing the Dimensionality of the Problem

The dimensionality of the least-squares problem grows as $3n$, where n is the total number of UAVs in the formation. As a result, the minimisation procedure does not scale well for large formations. The LS method solves this problem by reducing the number of UAVs required for the flux calculation by considering only the UAVs on the boundary of S_1 . This has the huge advantage that the scheme can be extended to many UAVs without any decrease in performance whilst preserving the flux calculation over the whole surface. Note that while leader-follower methods can also use rigid constraints between UAVs to reduce the dimensionality of the path planning, this results in a formation that cannot orientate itself toward a target.

The reduction in dimensionality of the planning can be shown by considering Gauss's law for electric fields given by:

$$\iint_S \mathbf{E} \cdot \hat{\mathbf{n}} dA = \frac{Q}{\epsilon_0} \quad (5)$$

where \mathbf{E} is the electric field, dA is an infinitesimal area on the Gaussian surface, $\hat{\mathbf{n}}$ is the unit normal to the surface, Q is the charge, and ϵ_0 is the free-space dielectric permittivity.

The law states that the flux through a closed surface is equal proportional to the enclosed charge, Q and the flux. However, in this problem, the flux through the closed surface is zero, since the charged target is outside of the surface shown in Figure 1. Splitting the integral across the surface S_1 , Equation 6, and S_2 , we find the magnitudes of flux through S_1 and S_2 . Thus, the flux can be computing using only the boundary UAVs $\mathbf{p}_1, \mathbf{p}_2, \mathbf{p}_3, \mathbf{p}_4$. This has the important result that the minimisation in the problem only ever depends on the position of 4 UAVs. Technically 3 UAVs can be used but the approximation of a hemisphere is poorer:

$$\iint_{S_1} \mathbf{E} \cdot \hat{\mathbf{n}} dA + \iint_{S_2} \mathbf{E} \cdot \hat{\mathbf{n}} dA = 0 \quad (6)$$

$$|\Phi_1| = |\Phi_2| \quad (7)$$

III. CONSTRAINTS FOR FORMATION PLANNING

In this section, we will first discuss the improvements we made to the LS method to make it more effective for UAV path prediction. Next, the new FG method which also uses the flux through the formation to generate UAV trajectories will be presented.

A. LS Modification

The drawback of the LS method is that the formation increases in size at each iteration. This is because a larger surface area also increases the flux. This effect was not seen in previous work since the distance from the cloak to the target was small. To solve this problem, we propose adding

an additional term to Equation 4 to control the size of the formation:

$$J(\Delta x) = \Delta x^T \Delta x + \alpha(\phi_r - J_\phi \Delta x)^2 + \beta(A \Delta x)^2, \quad (8)$$

where β is a soft constraint for the position retention term, A is:

$$A = \begin{pmatrix} B & 0 & 0 \\ 0 & B & 0 \\ 0 & 0 & B \end{pmatrix}, \quad (9)$$

where B is:

$$B = \begin{pmatrix} 1 & -1 & 0 & 0 \\ 0 & 1 & -1 & 0 \\ 0 & 0 & 1 & -1 \\ -1 & 0 & 0 & 1 \end{pmatrix}, \quad (10)$$

Differentiating Equation 8 and setting the result equal to zero produce the following linear problem:

$$(1 + \alpha J_\phi^T J_\phi + \beta A^T A) \Delta x = \alpha J_\phi^T \phi_r \quad (11)$$

B. Target Modelling

FG considers two types of target. The first is a single target and the second is a distribution of discrete targets. These models are useful for tracking objects which are not distributed continuously, such as swarms of UAVs. However, for geometric complex targets, an approximate charge distribution can be determined by considering an equivalent set of discrete charges which produce an equipotential at the surface of the target [4].

A single target is modelled as a single charge and therefore the contribution of the flux through a triangle in S_2 is given by Equation 2. For multiple targets, it is possible to use several point charges and sum the contribution of each to the flux through each triangle. However, a more efficient approach is to consider the centre of charge of the targets and determine an effective radius of the formation based on the maximum relative distance of a target in the swarm with respect to the centre of the charge. In the centre of charge case, the objective function is faster to compute since only a single charge contributes to the total flux.

C. Flux Guided Method

LS considers the iterative solution to a regularised linear least-squares problem to solve the path planning problem. In contrast, we solve the flux minimisation problem directly without the least-squares cost function assumption in FG. This eliminates the idea of a target flux value and allows the introduction of constraints for the UAV formation positions.

Once an expression of the total flux through the surface S_1 is found, the positions of the UAVs which increase the flux through the surface can be found by minimising the function $\Phi_2(x)$. In particular, we define the problem as obtaining the minimum of the negative flux. Specifically, for a surface normal $\hat{\mathbf{n}}$ as in Figure 1, the flux is negative, and decreases in the negative direction as the surface moves toward the target. When the unit vector is reversed the flux is positive but has the same magnitude. Therefore by finding the negative flux

we obtain a solution in which the formation is orientated toward the target.

Many potential solutions to the flux minimisation problem are not suitable for threat mitigation. For instance, the flux can be increased by simply expanding the formation. This solution is not suitable since we require the formation to surround the formation at a given distance. Also, many local solutions about the target exist. For example, any hemisphere rotated about the target is a solution.

Instead, we prefer to apply some constraints to directly limit our solution to a feasible set. Primarily, we wish to limit the size of the formation. Therefore, we impose quadratic equality constraints that limit the absolute length of the side-length of the boundary.

Whilst these constraints permit a rhombic formation of the leaders, the overall flux minimisation should ensure that the formation remains square since the flux is greatest when the formation area is maximised. More stringent conditions were placed on the dot products of the vectors between the leader UAVs; however, these were overly restrictive as they resulted in extremely slow convergence.

The primary advantage of this constraint formulation is the absolute length of formation edges is preserved throughout the minimisation. This means the solution at each iteration is collision-free. Also, since that relative motion of the formation is not constrained, the system can perform complex manoeuvres to align itself with and navigate toward the target. Also, the final size of the formation can be set by specifying the final side-length, l in the constraints.

We formulate the flux minimisation problem as:

$$\begin{aligned} & \underset{\mathbf{x} \in \mathbb{R}^{12}}{\text{minimize}} && \Phi_2(\mathbf{x}) \\ & \text{subject to} && (\mathbf{p}_1 - \mathbf{p}_2)^T (\mathbf{p}_1 - \mathbf{p}_2) = l^2 \\ & && (\mathbf{p}_2 - \mathbf{p}_3)^T (\mathbf{p}_2 - \mathbf{p}_3) = l^2 \\ & && (\mathbf{p}_3 - \mathbf{p}_4)^T (\mathbf{p}_3 - \mathbf{p}_4) = l^2 \\ & && (\mathbf{p}_4 - \mathbf{p}_1)^T (\mathbf{p}_4 - \mathbf{p}_1) = l^2, \end{aligned} \quad (12)$$

where

$$\mathbf{p}_1 = (x_1, x_2, x_3)^T \quad (13)$$

$$\mathbf{p}_2 = (x_4, x_5, x_6)^T \quad (14)$$

$$\mathbf{p}_3 = (x_7, x_8, x_9)^T \quad (15)$$

$$\mathbf{p}_4 = (x_{10}, x_{11}, x_{12})^T, \quad (16)$$

where $\mathbf{p}_1, \mathbf{p}_2, \mathbf{p}_3, \mathbf{p}_4$ are the position vectors of leader UAVs in Figure 1.

Equation 12 forms a non-linear optimisation programming problem with quadratic constraints. This type of problem can be solved using sequential quadratic programming (SQP) with equality constraints. SQP algorithms are implemented in many programming languages. We have chosen to use a Python implementation, *trust-constr*, available from the SciPy Python package.

IV. EXPERIMENTAL RESULTS

The following experiments show the results of the motion planning generated by the FG method. In each experiment, a hemispherical formation of UAVs is defined by specifying the positions of the four UAVs on the open surface's boundary as shown in Figure 1. The target and its radius are specified as inputs to the path planning algorithm. These parameters form the basis of the high-level control mechanism.

Four experiments are set up for different analysis. In the first one, we compare the paths planned by the FG, LS, and the LS with an additional soft constraint. In the second one, we show the results of the formation control problem for tracking a single target. In the third one, we show efficient multiple target tracking using the centre of charge approach, and in the fourth one, we demonstrate the path planning for the entire formation whilst generating paths only for the leader UAVS. The details are presented in the following subsections.

A. Comparison of Path Planning

In the first experiment, we compare the path planning between the flux guided method and the least-squares approach. A square formation facing in the $\hat{\mathbf{i}}$ direction is considered. The UAVs are positioned at $\mathbf{p}_1 = (0, 0, 0)$, $\mathbf{p}_2 = (0, 5, 0)$, $\mathbf{p}_3 = (0, 5, 5)$, $\mathbf{p}_4 = (0, 5, 5)$ and the target is positioned at $\mathbf{t} = (40, 40, 40)$, and $\alpha = 1000$ and $\beta = 0, 400$.

Figure 2 shows the paths generated by the FG and the LS. Each method results in smooth, non-colliding paths which surround the target. Surrounding is defined as the flux through the surface reaching a maximum. The LS, $\beta = 0$ case yields a path that greatly increases the formation's size. This result is unsuitable where the formation should be maintained in size, or the final positions of the UAVs should be close to the target. Also, for time parameterisation, the traversal time will be greater. In the $\beta = 400$ case, the formation retains its shape however the path is arc-shaped. Other values of β did not result in straighter paths. The path is arc-shaped because the rotation of the formation is suppressed by the β constraint. For example, two opposing UAVs cannot move independently of the two remaining UAVs, since their change in direction must be close to equal. This effect limits the range of motion of the formation significantly. The FG example shows the formation produces an initially rotation and then tracks directly toward the target. This spatially efficient path is possible since only the distance between each UAV is constrained. In addition, straighter paths are preferred since less acceleration is required in comparison with curved paths. Table I shows the combined path length for each UAV in the formation. The LS $\beta = 400$ and the FG plan paths which are ≈ 100 m shorter than the original formulation.

In each case, the formation retains its square shape even though the angles between the UAVs are unconstrained. The reason for this is that the square occupies the maximum area for a quadrilateral and therefore the flux through it is a maximum. Where other formation shapes are desired, such as

rhombus, the angles between the UAVs must be constrained since the flux through the surface is sub-optimal.

Figure 3 shows the planned paths when the target is placed at $\mathbf{t} = (-40, 0, 0)$. In this case, the formation is facing away from the target. The $\beta = 400$ case now performs a more exaggerated arc, and the formation surrounds the target without rotation. In contrast, the formation in the FG performs a rotation about \mathbf{p}_2 , \mathbf{p}_4 and tracks the target in a straight line. Table I shows that the FG path is $1.4\times$ shorter than the original formulation, and $1.5\times$ shorter than the soft constrained formulation. This shows that the FG is particularly successful when the formation faces away from the target.

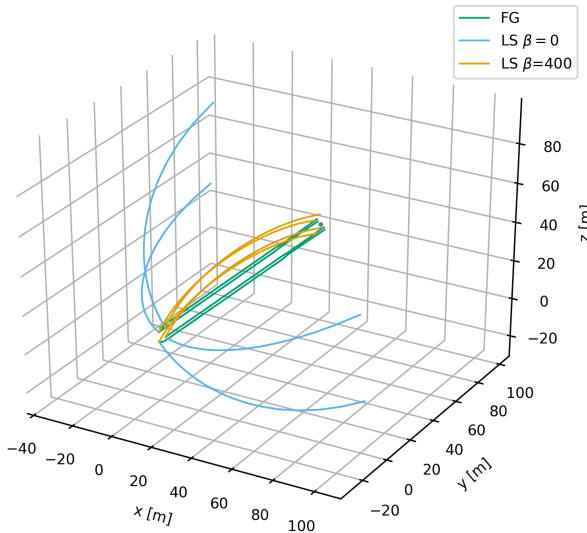


Fig. 2: Comparison of path planning for the Flux Guided, and least-squared methods for $\beta = 0, 400$

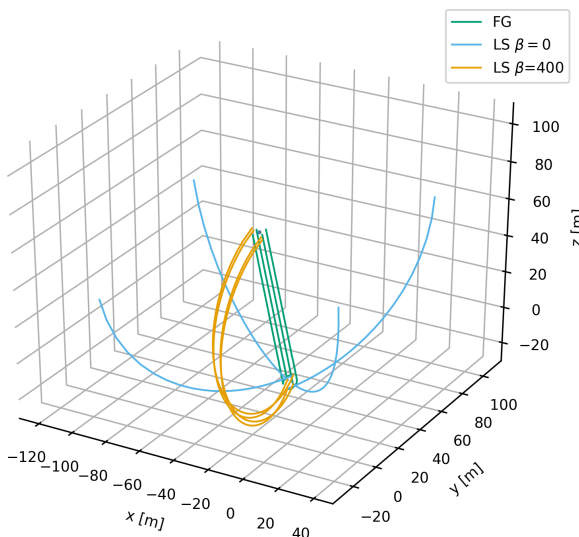


Fig. 3: Comparison of path planning for the Flux Guided, and least-squared methods for $\beta = 0, 400$

Target [m]	LS $\beta = 0$ [m]	LS $\beta = 400$ [m]	FG [m]
(40, 40, 40)	455	346	345
(-40, 40, 40)	500	543	354

TABLE I: Comparison of the combined path lengths for the UAVs in the square formation given by the FG, and LS $\beta = 0, 400$ path planning algorithms.

B. Tracking a Single Object

In this subsection, we derive time-optimal trajectories with performance constraints for the geometric paths obtained in the previous subsection, subsequently, the trajectories are simulated using a 3d dynamic particle simulation and evaluated against the performance constraints.

The FG generates a series of 3d points which form the geometric shape of the paths taken by leader UAVs. Each set of points generated at each iteration of the minimisation are collocated in time. Thus the formation movement is synchronised. The paths must be re-parameterised in time such that a reference trajectory for a robot can be determined. The re-parameterisation of the path is obtained using a Time-Optimal Path Parameterisation (TOPP) [17]. TOPP allows performance constraints to be given to the re-parameterisation of the path such that physically realisable trajectories can be obtained. Performance constraints of $|\mathbf{v}| = 10 \text{ ms}^{-1}$, and $|\mathbf{a}| = 5 \text{ ms}^{-2}$ are chosen. Since SQP does not guarantee that the path is smooth some filtering is applied to the path to remove points that are closely spaced prior to the trajectory generation. This was found to improve the efficiency of the TOPP.

To track the trajectory a 3d particle simulation, $\mathbf{a} = \mathbf{u}$, is used with the discrete dynamics:

$$\begin{pmatrix} \mathbf{x}(n+1) \\ \mathbf{v}(n+1) \end{pmatrix} = \begin{pmatrix} 1 & \Delta t \\ 0 & 1 \end{pmatrix} \begin{pmatrix} \mathbf{x}(n) \\ \mathbf{v}(n) \end{pmatrix} + \begin{pmatrix} \frac{1}{2} \Delta t^2 \\ \Delta t \end{pmatrix} \mathbf{u}(n), \quad (17)$$

where $\mathbf{x}(n)$, $\mathbf{v}(n)$ are the 3d position and velocity states at $t = n\Delta t$, and $\mathbf{u}(t)$ is the applied control force. The control force is generated by a PID controller which tracks the trajectory generated by the FG.

Figure 4 shows a comparison of the filtered path generated by the FG and the trajectory followed by the particle in the simulation. A square formation is used and the initial positions are the same as in the previous experiments. A target is placed at $\mathbf{t} = (40, 40, 40)$ m. The figure shows that the particle follows the desired trajectory with little deviation from the desired path. Figure 5 shows the velocity and acceleration of each particle over the duration of the simulation. Since the dynamic model is linear it is expected that the trajectory of the particle will always converge to the desired path if a large enough control force is used. However, the figure shows that the acceleration and hence the control forces are always within the performance constraints. In addition, the velocity curve is within the performance constraints and is relatively smooth. The blue squares along the trajectory show the shape of the formation during the simulation. The formation remains square throughout the duration of the simulation.

Figure 6 repeats the previous experiment with the exception that the target is positioned at $\mathbf{t} = (-20, 20, 20)$ m. The figure shows that the trajectories of the particles deviated only slightly from the desired path. The formation remains intact throughout the duration of the simulation. In particular, the formation remains square during the rotation manoeuvre at the start of the simulation. Figure 7 shows that the particle remains within the given performance constraints and that the velocity of the particle is quite smooth.

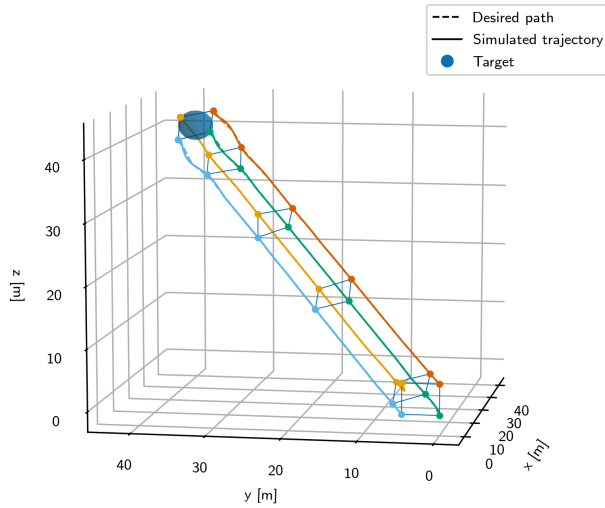


Fig. 4: Comparison of the simulated trajectory and the desired path for leaders in a square formation tracking a target at $(40, 40, 40)$.

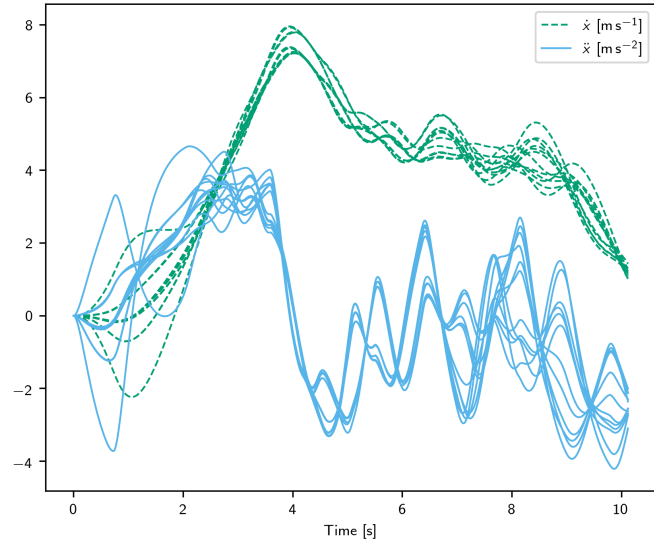


Fig. 5: Simulated velocity and acceleration curves for leaders in a square formation tracking a target positioned at $(40, 40, 40)$

C. Tracking Multiple Objects

An advantage of the FG approach in comparison to the LS approach is that it can control the scale of the formation.

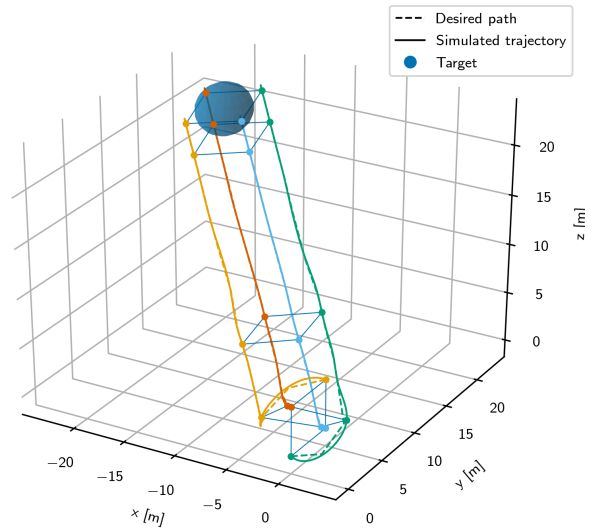


Fig. 6: Comparison of the simulated trajectory and the desired path for leaders in a square formation tracking a target at $(-20, 20, 20)$.

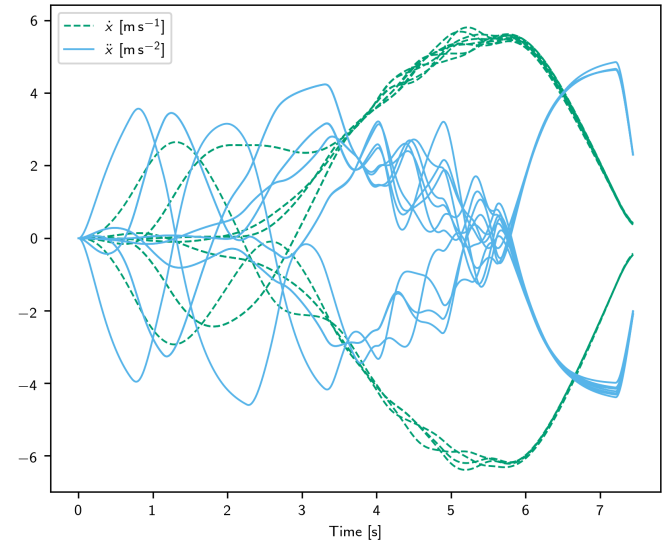


Fig. 7: Simulated velocity and acceleration curves for leaders in a square formation tracking a target positioned at $(-20, 20, 20)$

An application of this property is that the formation can be guided to cover several targets or guided to the location of a target that has some uncertainty in its position. The approach is computationally efficient since it only considers the location of the centre of charge (COC) as a source of radiation, and an effective radius given by the distance from the outermost target to the COC. The COC is defined as the average of the target positions. To show the flexibility of this approach, the positions of the targets are drawn from a normal distribution. By altering the parameterisation of the distribution we show that the FG can respond to varied scenarios or levels of uncertainty in the position of the target.

Figure 8 shows the trajectories simulated by the FG. The

positions of 10 targets are drawn from a normal distribution parameterised by $N(\mu = 200, \sigma = 100)$ shown in grey. The starting positions of the formation are the same as the previous experiment. The results show that the leaders successfully locate and optimally surround the target formation. The figure shows the formation and the target formation at four-time steps. At each time-step, the formation retains its shape. The final position of the formation maximises the coverage of the total charge of the targets.

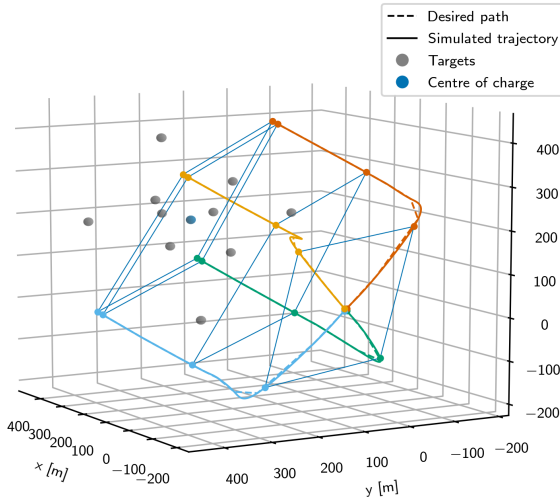


Fig. 8: Comparison of the simulated trajectories and desired paths of leaders in a square formation. The formation scales and rotates such that targets are surrounded centred at the centre of charge.

D. Formation Motion

A key advantage of the FG planning algorithm is that number of degrees of freedom is drastically reduced since only the nodes on the boundary of the open surface area required for the flux calculation. This has the result that a complex formation on the boundary can be planned whilst only considering a subset of nodes.

Here, we simulate the motion of the hemisphere shown in Figure 1 toward a target positioned at $\mathbf{t} = (10, 10, 10)$. The FG plans trajectories for the leader UAVs \mathbf{p}_1 , \mathbf{p}_2 , \mathbf{p}_3 , \mathbf{p}_4 . The paths of the follower UAVs are derived from the leaders using vector algebra. In leader/follower schemes this is also the case however in the FG can plan trajectories where the formation direction is not in the direction of motion. In most leader/follower schemes, the velocity defines the orientation of the formation. The derivation of these paths is computationally trivial. Once all the paths are obtained they are parameterised using TOPP and the previous performance constraints. Figure 9 shows the motion of the formation toward the target at the beginning, end and two intermediate stages of the flight. Also shown are the desired paths and simulated trajectories of each UAV. The figure shows the formation maintains its shape for the duration of the flight.

In addition, the formation optimally surrounds its target. In summary, experimental results have shown that for followers and leaders velocity and acceleration are bounded by the performance constraints, and the velocity profile is smooth.

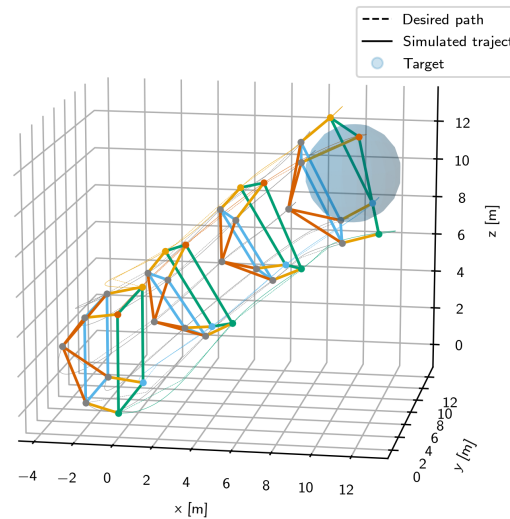


Fig. 9: Simulation of a hemispherical formation surrounding a remote target. The leader UAVs are represented as coloured markers and the followers are in grey. The formation covers the target whilst maintaining its formation. Only the leader UAVs require path planning.

In the next experiment, the same methodology is used and the target is positioned at $\mathbf{t} = (-10, 10, 10)$. Figure 10 shows the formation at three different time steps. The formation retains its shape during the flight, and acts to maximise its coverage of the target at all time. Separate tests have shown that the followers perform within the performance constraints and the velocity profile is smooth.

V. CONCLUSIONS AND FUTURE WORK

We have demonstrated a new formulation for the path planning of UAVs using a harmonic electric field. The formulation plans paths for trajectories of UAV in hemispherical formations toward a target whilst maintaining the shape of the formation. In particular, the orientation of the formation is not governed by the velocity of the leader UAV as in many leader/follower schemes. This has the advantage that the formation always acts to face the target without altering its shape.

The new formulation has several advantages over previous formulations. Firstly, the formation retains its shape over the entirety of the path planning. Secondly, the total path length of the planned path is significantly lower. This is advantageous as the magnitude of the control force is reduced, and the total distance travelled is shorter. Thirdly, the scale of the formation can be controlled. This allows groups of targets to be tracked, or uncertainty in the target location to be taken into account. Also, the scheme retains the novel property

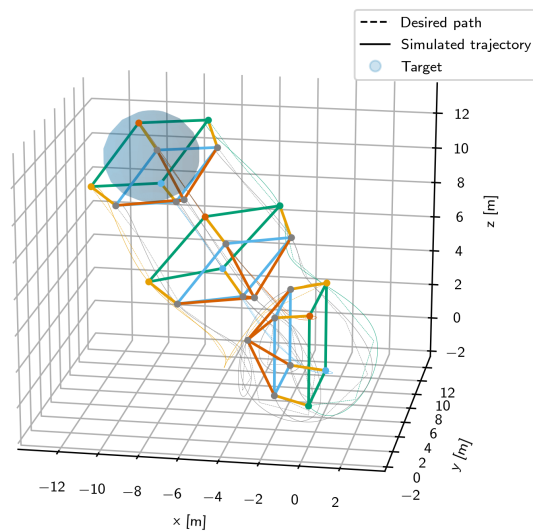


Fig. 10: Simulation of a hemispherical formation surrounding a remote target that is positioned behind the formation's open face. The formation rotates itself and subsequently surrounds the target.

that only UAVs on the open boundary of the surface require planning which makes it highly scalable.

We have also demonstrated that the generated paths can be used for generating smooth trajectories for robotic applications. And that these trajectories can be followed by a 3d dynamic particle system using a PID controller.

While this paper presents a new approach for controlling formation for UAVs and demonstrates its effectiveness, the trajectory generation has not been applied to moving targets. Since the method is based on path planning, the entire path to the target must be calculated to the target every time the target position is updated. This is because we do not know a priori the distance along the path the drone will reach. Nevertheless, the solve time for the minimisation is small for reasonable numbers of drones and thus the algorithm should be able to be applied to a number of realistic cases.

Besides, the trajectory generation system proposed in this work has been developed for DJI drones API. As such the scheme can experimentally be validated by outdoor testing which is one of the future directions the team is currently working on.

REFERENCES

- [1] Y. Lu, Z. Xue, G.-S. Xia, and L. Zhang, "A survey on vision-based uav navigation," *Geo-spatial Information Science*, vol. 21, no. 1, pp. 21–32, 2018.
- [2] O. Khatib, "Real-time obstacle avoidance for manipulators and mobile robots," in *Proceedings. 1985 IEEE International Conference on Robotics and Automation*, vol. 2, pp. 500–505, Institute of Electrical and Electronics Engineers, 1985.
- [3] T. Paul, T. R. Krogstad, and J. T. Gravdahl, "Modelling of UAV formation flight using 3D potential field," *Simulation Modelling Practice and Theory*, vol. 16, no. 9, pp. 1453–1462, 2008.
- [4] J. Wang, X. Wu, and Z. Xu, "Potential-based obstacle avoidance in formation control," *Journal of Control Theory and Applications*, vol. 6, pp. 311–316, aug 2008.

- [5] Y. Kuriki and T. Namerikawa, "Consensus-based cooperative formation control with collision avoidance for a multi-UAV system," in *2014 American Control Conference*, pp. 2077–2082, jun 2014.
- [6] Y. Chen, J. Yu, X. Su, and G. Luo, "Path Planning for Multi-UAV Formation," *Journal of Intelligent & Robotic Systems*, vol. 77, no. 1, pp. 229–246, 2015.
- [7] F. Janabi Sharifi and D. Vinke, "Integration of the artificial potential field approach with simulated annealing for robot path planning," pp. 536–541, 1993.
- [8] Min Gyu Park, Jae Hyun Jeon, and Min Cheol Lee, "Obstacle avoidance for mobile robots using artificial potential field approach with simulated annealing," in *ISIE 2001. 2001 IEEE International Symposium on Industrial Electronics Proceedings (Cat. No.01TH8570)*, vol. 3, pp. 1530–1535, IEEE, 2001.
- [9] Q. Zhu, Y. Yan, and Z. Xing, "Robot path planning based on artificial potential field approach with simulated annealing," *Proceedings - ISDA 2006: Sixth International Conference on Intelligent Systems Design and Applications*, vol. 2, pp. 622–627, 2006.
- [10] K. H. Kowdiki, R. K. Barai, and S. Bhattacharya, "Leader-follower formation control using artificial potential functions: A kinematic approach," *IEEE-International Conference on Advances in Engineering, Science and Management, ICAESM-2012*, pp. 500–505, 2012.
- [11] J. Zhang, J. Yan, and P. Zhang, "Fixed-wing UAV formation control design with collision avoidance based on an improved artificial potential field," *IEEE Access*, vol. 6, pp. 78342–78351, 2018.
- [12] N. E. Leonard and E. Fiorelli, "Virtual leaders, artificial potentials and coordinated control of groups," in *Proceedings of the 40th IEEE Conference on Decision and Control (Cat. No.01CH37228)*, vol. 3, pp. 2968–2973 vol.3, 2001.
- [13] L. He, P. Bai, X. Liang, J. Zhang, and W. Wang, "Feedback formation control of UAV swarm with multiple implicit leaders," *Aerospace Science and Technology*, vol. 72, pp. 327–334, 2018.
- [14] D. Morgan, G. P. Subramanian, S.-J. Chung, and F. Y. Hadaegh, "Swarm assignment and trajectory optimization using variable-swarm, distributed auction assignment and sequential convex programming," *The International Journal of Robotics Research*, vol. 35, pp. 1261–1285, sep 2016.
- [15] H. Wang, K. A. Sidorov, P. Sandilands, and T. Komura, "Harmonic parameterization by electrostatics," *ACM Transactions on Graphics*, vol. 32, no. 5, 2013.
- [16] A. Van Oosterom and J. Strackee, "The Solid Angle of a Plane Triangle," *IEEE Transactions on Biomedical Engineering*, vol. BME-30, pp. 125–126, feb 1983.
- [17] H. Pham and Q. C. Pham, "A new approach to time-optimal path parameterization based on reachability analysis," *IEEE Transactions on Robotics*, vol. 34, pp. 645 – 659, 06 2018.